Sputtering pressure dependence of hydrogen-sensing effect of palladium films

Chung Wo Ong[a] and Yu Ming Tang
Department of Applied Physics and Materials Research Center, The Hong Kong Polytechnic University, Hung Hom, Kowloon, Hong Kong, People's Republic of China

(Received 11 August 2008; accepted 6 January 2009)

The electrical resistivity ρ of palladium (Pd) films prepared by using magnetron sputtering at different pressures ϕ ranging from 2 to 15 mTorr showed very different hydrogen (H)-induced response. This is because the mean free path of the particles in vacuum changes substantially with ϕ, such that the structure of the deposits is altered accordingly. A film prepared at a moderate ϕ value of 6 mTorr has a moderate strength. After a few hydrogenation-dehydrogenation cycles, some cracks are generated because of the great difference in the specific volumes of the metal and hydride phases. Breathing of the cracks in subsequent switching cycles occurred, which led to the response gain of ρ, defined as the resistivity ratio of the dehydrogenated-to-hydrogenated states during a cycle, to increase to 17. This result demonstrates the attractiveness of using the Pd films in H_2 detection application. The H-induced resistive response of the films prepared at higher or lower ϕ values was found to be much smaller.

I. INTRODUCTION

Palladium (Pd) can dissociate hydrogen molecules (H_2) and absorb H atoms at room temperature to result in a remarkable change in electrical resistivity (ρ).[1] This effect becomes more attractive due to a great variety of the demands on H_2 detection.[2–4] When a small amount of H atoms is incorporated into Pd, a metal-hydride α-phase is first produced. The resistivity ρ would increase to approximately 1.05 times that of the pure metal phase ρ_o. A further increase in H content leads to nucleation of a metal-hydride β-phase.[5] The value of ρ would increase further to 1.6 to 1.8 times of ρ_o when the H content is increased to 65 to 75 at.%.[6] This effect is primarily attributed to the difference of the ρ values between the metal phase and the hydride phase. The effect has been used for making H_2 sensors, in which the sensing elements are in the form of Pd wires or thin films.[7,8] Typical resistive change based on this mechanism is approximately 0.5 to 8% in an environment containing 1 to 5% of H_2. In general, the response time is in the order of 10 to 20 s.

More recently, Pd made to have a defective structure containing pores/defects was found to be able to produce a much higher and faster resistive response to H_2 based on a different mechanism. One distinctive feature of a response based on such a mechanism is that the direction of the change of ρ is opposite to that of the foresaid one. This is because the lattice constants of pure Pd metal and the metal-hydride β-phase are in the ranges of 0.3889–0.3890 and 0.4013–0.4025 nm, respectively,[9] i.e., a mean difference of 3.3%, such that full hydrogenation of pure metal Pd is estimated to give a volume increase by 10%. As a consequence, some pores/defects in the structure could be closed to result in a rapid drop of ρ.[10–12] The opposite occurs during dehydrogenation. This mechanism is referred to as the hydrogen-induced-volume-change effect (HIVC) in this article. Studies on this topic are greatly stimulated by the recent development of nanofabrication technology. Some important examples are as follows. Pd mesowires subjected to a biased voltage of 5 mV applied along the length direction showed a rapid current change to 8 μA from a negligible level in a period of 75 ms after being exposed to an ambient containing 10% of H_2.[13] A film consisting of agglomerated Pd clusters gave a 50% drop of ρ when it was put in an H_2 atmosphere at a pressure of 9×10^4 Pa.[14] An ultrathin film made by depositing nanosized Pd clusters on a siloxane-coated silicon substrate exhibited a 60% drop of ρ in 70 ms when it was placed in an environment containing 2% of H_2.[15] However, it was also shown in an example that this mechanism cannot be activated although some nanosized features were introduced in the fabrication process by depositing a Pd film on an anodic oxidized aluminium substrate. Its ρ value just showed a 15% change and increased during hydrogenation and dropped during dehydrogenation.[16]

The present study was carried out based on the theory that the structure of a film prepared by using magnetron sputtering was sensitive to the setting of the vacuum

[a]Address all correspondence to this author.
e-mail: apacwong@inet.polyu.edu.hk
DOI: 10.1557/JMR.2009.0238

pressure ϕ. According to the kinetic theory of gases, particles in a higher vacuum environment (low ϕ value) would have a longer average mean free path so that they can bombard the substrate surface with a higher average kinetic energy to produce a relatively dense film structure.[17] On the contrary, if the vacuum pressure increases, scattering among the particles in vacuum is more severe, such that the film structure produced would become more defective. We believe that with the use of magnetron sputtering, there is a value of ϕ, at which the Pd film deposited would have a maximum HIVC effect which dominates the H-induced response of ρ. This study was performed to justify this conjecture through investigating the ϕ dependence of the structure of magnetron sputtered Pd films and their resistive response to hydrogen.

II. EXPERIMENTAL METHODS

Deposition of Pd films was performed in a stainless steel vacuum chamber equipped with a magnetron sputtering gun. Argon (Ar) was admitted into the chamber by means of a mass flow controller. The flow rate of Ar gas was fixed at 20 sccm. The pressure ϕ in the chamber was varied in a range of 2 to 15 mTorr by controlling the pumping speed with a gate valve at the entrance of a diffusion pump. The substrate holder was rotated all the way during each deposition process to make sure that the thickness of the film was as uniform as possible. The substrate heater was not turned on. A 2-inch Pd target mounted on the magnetron sputtering gun was first presputtered at an ambient pressure of 70 mTorr for 5 min while the shutter remained closed. The ambient pressure was then reduced to the expected level, and then the shutter was opened to start deposition. Each run lasted for 30 min. The thicknesses of the films, *t*, were controlled to fall between 49 and 64 nm as listed in Table I.

We observed the film crystalline structure with an x-ray diffractometer (XRD) (Philips X'Pert system, Almelo, The Netherlands) equipped with a Cu Kα radiation source. The system was operated in the glancing-angle mode with the incident x-ray beam making an angle of 3° from the substrate surface to maximize the diffraction intensity. The surface morphology of the film samples was observed with a scanning electron microscope [field emission-scanning electron microscope (FE-SEM) JSM-6335F; JEOL, Herts, UK] and an atomic force microscope [(AFM) NanoScope IV; Veeco, Plainview, NY]. The root-mean-square roughness (z_{RMS}) of the film surfaces was derived from the AFM data.

The resistance *R* of a Pd film across two electrodes predeposited on a glass substrate was measured. A nominal electrical resistivity ρ was calculated based on the measured *R* value, i.e., the thickness and width of the film sample. The response of ρ to hydrogen was observed by immerging the film sample in a small stainless steel chamber filled up with a gaseous admixture of 15% H_2 balanced in Ar. This procedure lasted for 24 h and is referred to as a soaking process in this article. The sample was then exposed alternatively to air and the above H-containing gas admixture, with each step lasting for 10 min. This procedure is named the cyclic test in this article. The chamber was evacuated to rough vacuum with a rotary pump before admission of the other gas.

TABLE I. Thickness *t*, lattice spacing d_{111}, grain size D, root-mean-square roughness z_{RMS}, and as-deposited electrical resistivity ρ_o of Pd films deposited at various sputtering pressures ϕ.

ϕ (mTorr)	*t* (nm)	d_{111} (nm)	D (nm)	z_{RMS} (nm) as-deposited	z_{RMS} (nm) after six cycles	ρ_o (μΩ cm)
2	55	0.232	11.3	0.603	4.49	34.4
6	57	0.230	8.90	0.943	42.5	115
	57	0.231	9.20	0.965	35.8	99.4
10	49	0.229	6.04	1.77	—	120
15	64	0.228	5.26	2.04	13.5	265
Pd target	—	0.225	25.4	—	—	—

III. RESULTS AND DISCUSSIONS

A. ϕ dependence of Pd film structure

The observed ϕ dependence of film structure is summarized as follows. Figure 1 shows the XRD spectra of a polycrystalline Pd specimen and the Pd films deposited at various ϕ values ranging from 2 to 15 mTorr. The spectrum of the polycrystalline specimen contains the (111) and (200) peaks, but the spectra of all the film samples only contain the (111) peak. This finding indicates that the crystalline grains in the films are preferentially

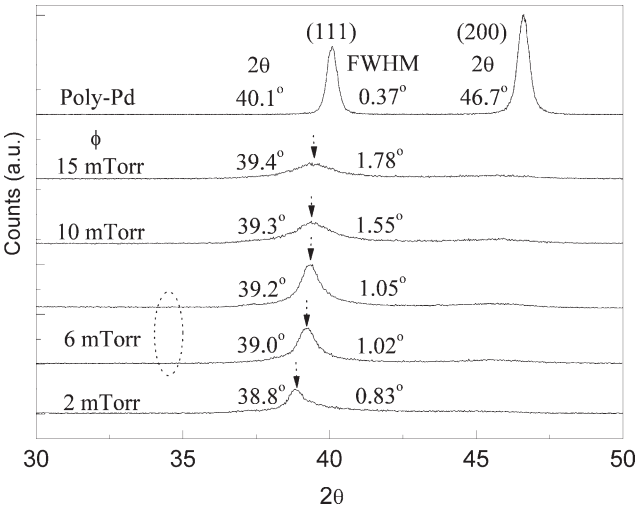

FIG. 1. XRD spectra of polycrystalline Pd (for reference) and Pd films deposited at various ϕ values.

orientated such that their (111) planes are basically in parallel with the substrate surface. Furthermore, with increasing ϕ, the (111) peak position shifts from 38.8 to 39.4°, and the full width at half maximum (FWHM) increases from 0.83 to 1.78°. The lattice spacing d_{111} is calculated to drop from 0.232 to 0.228 nm, and the average grain size D decreases from 11.3 to 5.26 nm [Table I and Figs. 2(a) and 2(b)]. SEM images of the film surfaces show that a film deposited at a higher ϕ value is rougher. Micrographs of two samples deposited at ϕ = 2 and 15 mTorr are given in Figs. 3(a) and 3(b) as examples. The values of z_{RMS} derived from the AFM profiles are found to increase from 0.603 to 2.04 nm [Table I and Fig. 2(c)].

To explain the above results, one refers to the kinetic theory of gases. It states that the mean free path λ of gas molecules depends on ϕ in the form of $\lambda = k_B T/(2^{1/2}\pi d^2 \phi)$, which can be expressed as $\lambda = 72.8/\phi$ (in cm), with k_B being the Boltzmann constant in SI unit, T the room temperature equal to 300K, *d* the diameter of an Ar molecule equal to 9.8×10^{-11} m, and ϕ in mTorr. When ϕ varies from 2 to 15 mTorr, the value of λ would vary from 36.4 to 4.85 cm, which covers the target-to-substrate distance of 8 cm used in our deposition processes.

Start from the condition of ϕ = 2 mTorr, where the mean free path of particles is longer than the target-to-substrate distance. Species sputtered from the target can travel through the vacuum to reach the substrate surface with little scattering. They carry energies in the order of a few tens of eV, which is a typical estimate for the particles involved in a sputtering process.[18] With energies in this range, atoms bombard on the substrate surface are closely parked to produce deposits of a relatively dense structure. Other than Pd atoms, some Ar atoms can intrude and incorporate in the deposits. The consequence is the induced in-plane compressive stresses in the film. We refer to Fig. 7 of Ref. 17 to support this argument, which shows that, in general, a thin film deposited by using techniques like magnetron sputtering, ion sputtering, and ion-assisted deposition involving particles with average kinetic energies of a few tens of eV or above would have compressive stresses. The in-plane compressive stresses and Ar intrusion can lead to an out-of-plane expansion, causing the lattice spacing of the planes in parallel to the substrate surface, namely d_{111} in this case, to be larger than that of the bulk material. This effect explains the observed result that the value of d_{111} of the film deposited at 2 mTorr is the largest among the samples. In addition, when particles of a few tens of eV land on the substrate surface, they are supposed to be rather mobile and can reach some lattice sites readily. This process favors the growth of larger crystallites, explaining the fact that the average grain size of the film deposited at 2 mTorr is larger than those deposited at higher ϕ values. We refer to an experimental fact to support this argument, which states that the structure of aluminum nitride films prepared by sputtering can be changed from being amorphous-like to

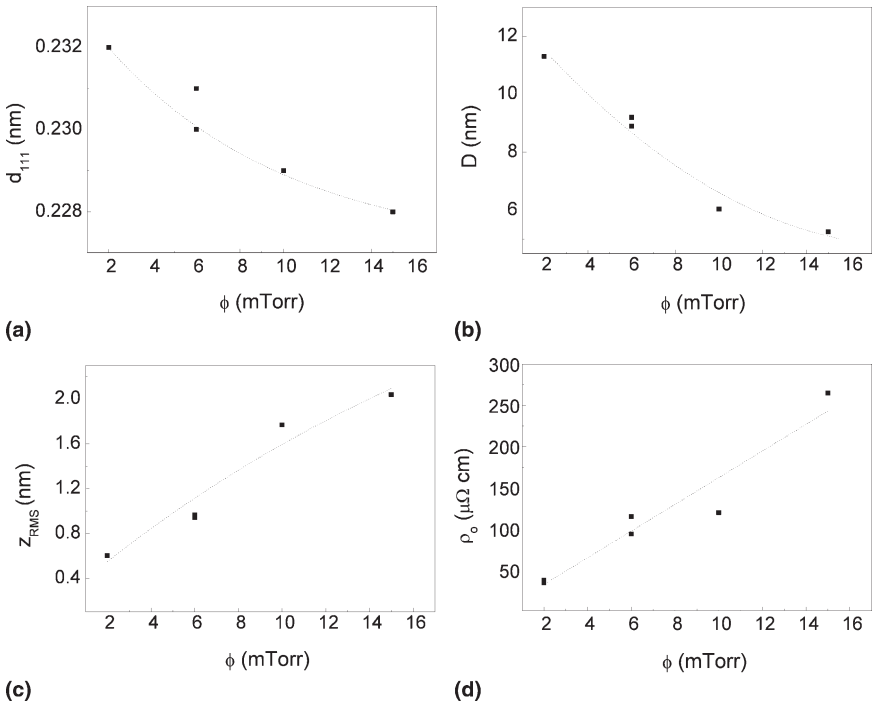

FIG. 2. Plots of (a) lattice spacing d_{111}, (b) grain size D, (c) root-mean-square roughness z_{RMS}, and (d) as-deposited electrical resistivity ρ_o against sputtering pressure ϕ.

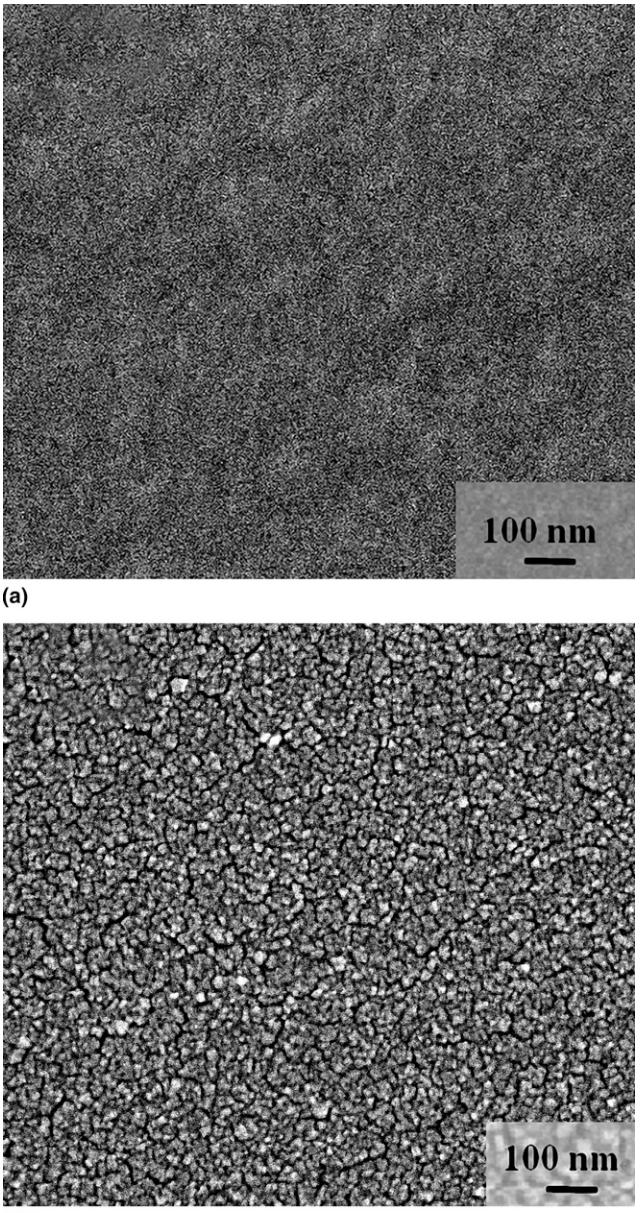

FIG. 3. SEM images of Pd films deposited at ϕ equal to (a) 2 mTorr and (b) 15 mTorr.

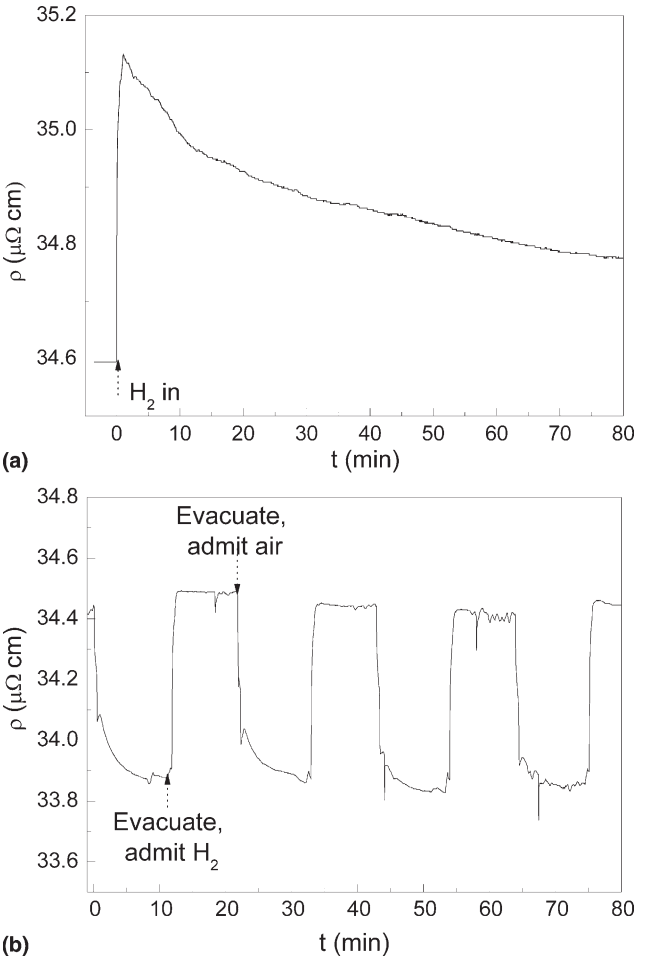

FIG. 4. The change of ρ of a Pd film deposited at 2 mTorr in (a) a socking process in 15% H_2 balanced in Ar; and (b) cyclic hydrogenation-dehydrogenation processes.

polycrystalline and then to epitaxial with successive increase in sputtering power, where the increase in sputtering power is supposed to lead to an increase in the mobility of the depositing particles.[19,20]

With the use of higher ϕ values, the average mean free path of particles in vacuum decreases to become comparable with or even shorter than the target-to-substrate distance. Particles sputtered from the target are scattered more severely such that their kinetic energies are thermalized to some extent before reaching the substrate surface. In addition, less Ar atoms can be injected into the deposits. Thus, the film structure produced is supposed to contain some defects or pores. One consequence is that the magnitude of internal stresses is lower. We refer to Fig. 7 of Ref. 17 to support this argument, which states that films deposited with techniques such as low-pressure or plasma-enhanced chemical vapor deposition involving particle energies in the range of 0.1 to a few tens of eV would have low compressive stresses or tensile stresses. This response alleviates the expansion of lattice spacing in the out-of-plane direction, so that a smaller d_{111} value is recorded for a film deposited at a higher ϕ value. In addition, because they have relatively low kinetic energies, depositing particles are less mobile. The size of the grains formed at an environment of a higher ϕ value is smaller. This result immediately explains two findings. First, film surface is rougher with increasing ϕ as reflected quantitatively by the increase in z_{RMS}. By referring to the surface morphology in Fig. 3(b), we further infer that the crystallites in a film deposited at ϕ = 15 mTorr tend to agglomerate in clusters. Second,

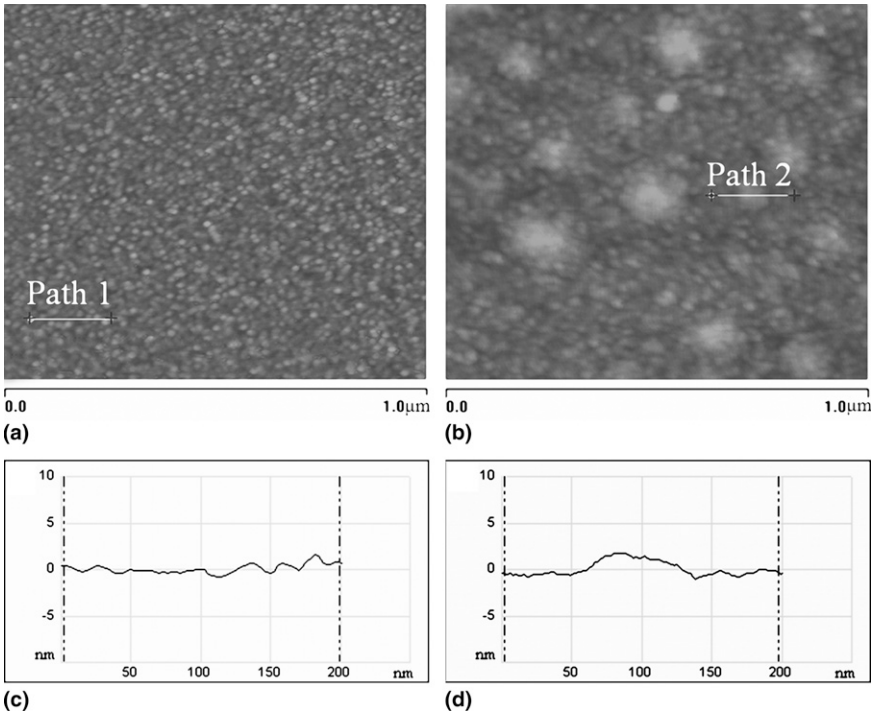

FIG. 5. Surface morphologies of a Pd film deposited at 2 mTorr (a) immediately after deposition and (b) after six hydrogenation-dehydrogenation cycles; and the corresponding profiles along (c) path 1 and (d) path 2, respectively.

the as-deposited nominal electrical resistivity ρ_o increases by 7.6 times from 34.8 to 265 μΩ cm when ϕ varies from 2 to 15 mTorr [Table I and Fig. 2(d)], because the film structure becomes more defective.

B. H-induced response of Pd films deposited at low ϕ of 2 mTorr

Consider the response of ρ of a film deposited at ϕ = 2 mTorr to the presence of hydrogen. Figure 4(a) shows the result in the soaking process. After H_2 is admitted to the measurement chamber, the value of ρ rises sharply to a peak value and then drops to approach some limit, where the dropping rate decreases as time proceeds. The time required to reach the steady state is longer than 80 min. We suggest that the initial rise of ρ is mainly due to the formation of a hydride phase, which is known to be more insulating than Pd metal. Hydrogenation causes the film material to have a tendency to expand, because the specific volume of the hydride phase is larger than that of the metal phase. However, any expansion in volume would cause the existing compressive stresses to further increase, such that the tendency of volume change is opposed. As such, the film structure would be self-modulated to approach a new equilibrium state by going through a relaxation process, which leads to the progressive drop in ρ as observed.

Figure 4(b) shows the change of ρ observed in the subsequent cyclic test. The value of ρ was found to rise during hydrogenation and drops during dehydrogenation. The fractional change of ρ and the rising time observed in a cycle are approximately 1.6% and 30 s, respectively, consistent with the typical features of H-induced resistive changes due to the reversible metal-hydride transitions and the difference between the electrical resistivities of the two phases.[7,8] Finally, we note that the AFM image of a freshly prepared sample [Fig. 5(a)] and that taken after six switching cycles [Fig. 5(b)] show that the film surface is just slightly roughened after the cyclic test, where the respective actual profiles are illustrated in Figs. 5(c) and 5(d): a completely different scenario is seen for the film deposited at higher ϕ values as described in the following.

C. H-induced response of Pd films deposited at moderate ϕ of 6 mTorr

The H-induced response of the films deposited at 6 mTorr shows distinctive features that are highly reproducible. Therefore, we only chose the data of two samples prepared at the same condition to present in this session.

Figure 6(a) shows the change of ρ of the two films in respective soaking processes, where the films were deposited at the same conditions but in two separate runs. When it is first brought into contact with H_2, the value of ρ shows a rapid drop and then slows down to approach some limit. This phenomenon can be explained if one

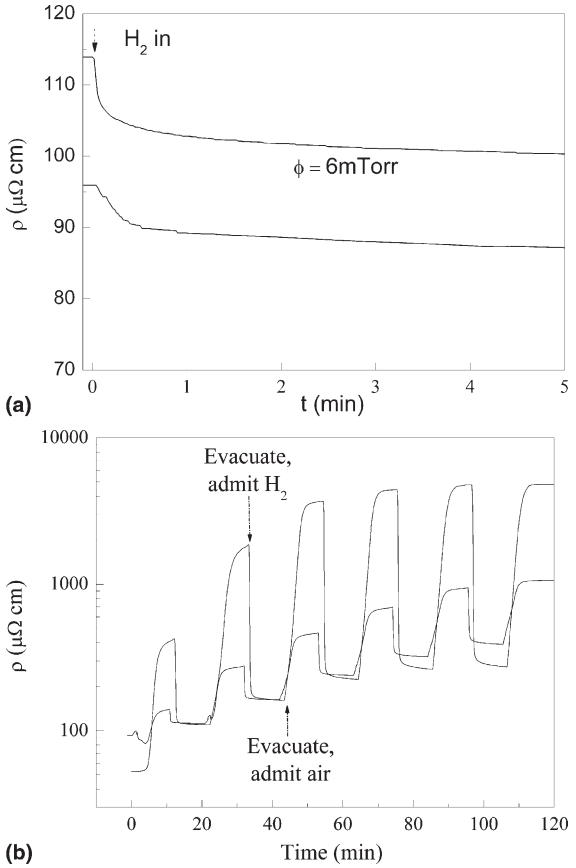

FIG. 6. The change of ρ of two Pd films deposited at 6 mTorr in (a) a socking process in 15% H_2 balanced in Ar; and (b) cyclic hydrogenation-dehydrogenation processes.

notices that the film deposited at this pressure is more defective than that deposited at a lower ϕ of 2 mTorr as pointed out in the previous section. One can thus assume that the film would contain some defects or pores. According to the HIVC effect, when it is hydrogenated in a soaking process, the film material tends to expand such that some of the defects or pores would be closed, and hence result in a lower apparent ρ value as observed.

Figure 6(b) shows the behaviors of ρ in the cyclic tests. Different from a sample deposited at 2 mTorr, the value of ρ of a film prepared at 6 mTorr drops during hydrogenation and rises during dehydrogenation, and the magnitude of the change is much larger (normally above 100%). In addition, at the initial stage of the test, the baseline drifts markedly, and the fractional change of ρ increases successively with the increasing number of switching cycles. However, after the first few cycles, the drift of the baseline slows down, and the fractional change of ρ in subsequent cycles becomes stable. It should also be noted that the fractional changes of ρ of different samples produced from two separate runs with the same condition can diversify in a broad range. For example, Fig. 6(b) shows that the response gains of ρ of two films prepared at the same ϕ value of 6 mTorr, defined as the resistivity ratio of the dehydrogenated-to-hydrogenated states in a cycle, rises to 2.5 and 17, respectively, after six switching cycles.

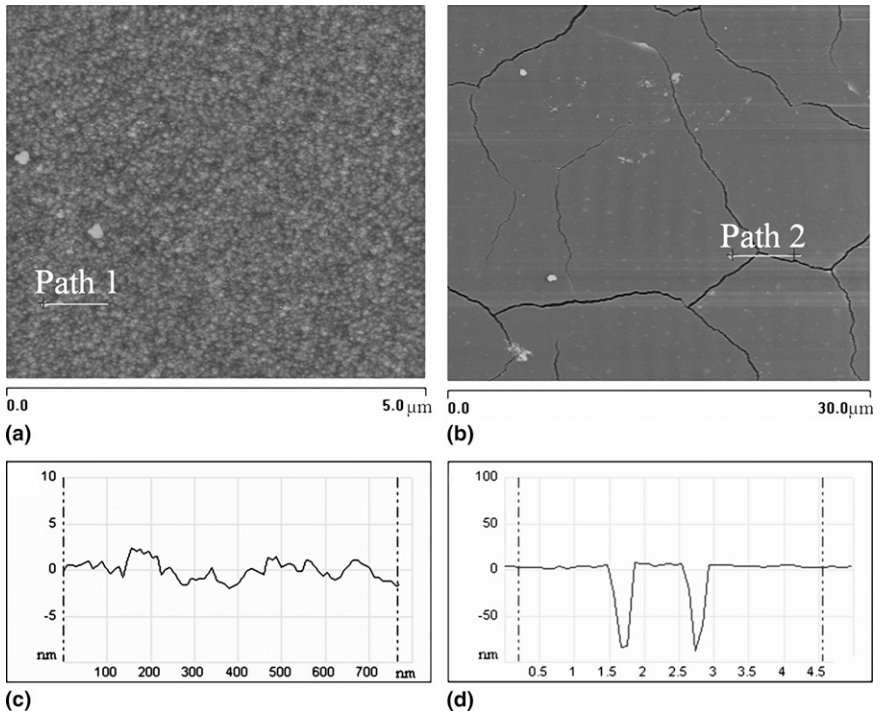

FIG. 7. Surface morphologies of a Pd film deposited at 6 mTorr (a) immediately after deposition and (b) after six hydrogenation-dehydrogenation cycles; and the corresponding profiles along (c) path 1 and (d) path 2, respectively.

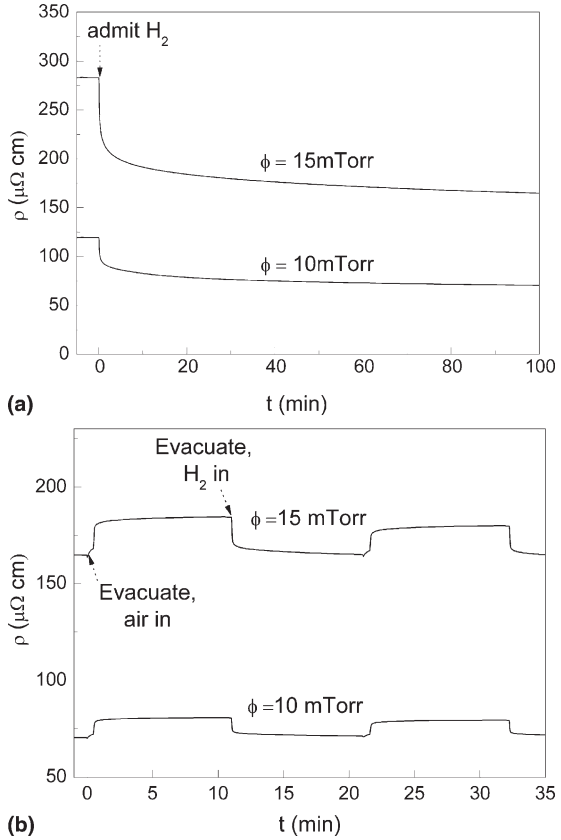

FIG. 8. The change of ρ of two Pd films deposited at 10 and 15 mTorr in (a) a socking process in 15% H_2 balanced in Ar; and (b) cyclic hydrogenation-dehydrogenation processes.

The above results can be understood if one compares the AFM images of a sample taken immediately after deposition [Fig. 7(a)] and after several switching cycles [Fig. 7(b)], with the respective actual profiles illustrated in Figs. 7(c) and 7(d). Figure 7(a) shows that the freshly prepared sample has a smooth surface. However, because the film structure is relatively defective and weak, repetitive volume expansions and contractions caused by hydrogenation and dehydrogenation processes lead to the generation of cracks as seen in Fig. 7(b). At this moment, the root-mean-square roughness z_{RMS} increases to 35.8 and 42.5 nm, respectively, from the common as-deposited level of 1 nm (Table I). Some of these cracks can be closed and opened in subsequent switching cycles—breathing effect. Thereby, the HIVC effect dominates the change of ρ. This effect explains the huge response of ρ and the direction of its changes when the film material interacts with hydrogen. Furthermore, the generation of the cracks should undergo an evolution process, which occurs mainly in the first few switching cycles. Meanwhile, the number and size of cracks keep increasing, such that the film structure at this stage is not stable. This result explains the drift of the baseline and the successive increase in the fractional change of ρ at the initial stage of a cyclic test. Considering that the HIVC effect can give a high sensitivity to the presence of H_2, it is worthy to search for an optimum condition where the resistive response is maximized and the structural instability is diminished to the minimum.

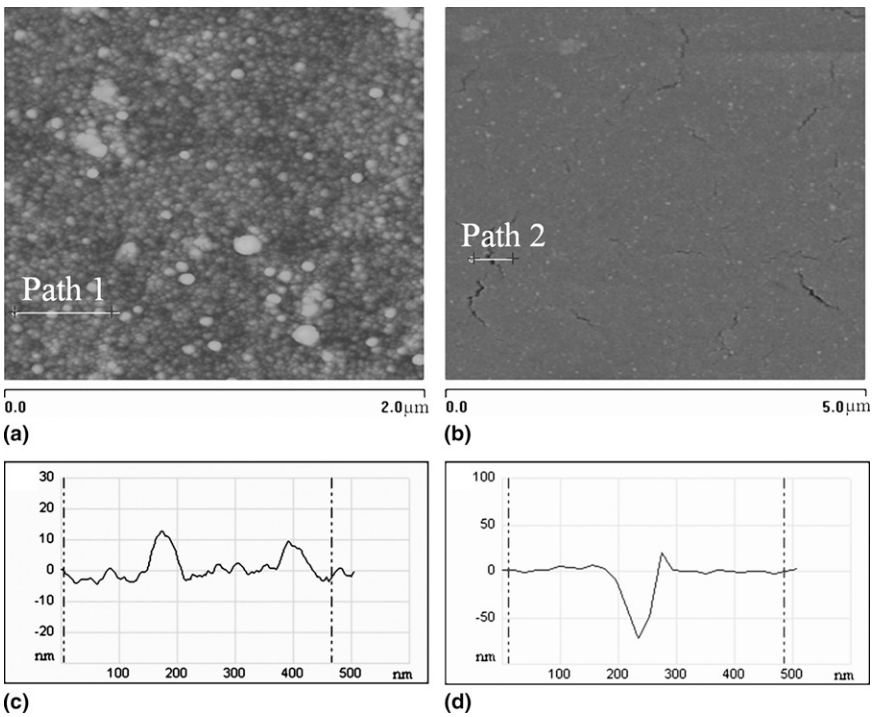

FIG. 9. Surface morphologies of a Pd film deposited at 15 mTorr (a) immediately after deposition and (b) six hydrogenation-dehydrogenation cycles; and the corresponding profiles along (c) path 1 and (d) path 2, respectively.

D. H-induced response of Pd films deposited at high ϕ of 10 and 15 mTorr

Figures 8(a) and 8(b) show the response of ρ to H_2 in the soaking and cyclic processes, respectively, for the samples deposited at ϕ = 10 and 15 mTorr. Results show that the value of ρ drops during hydrogenation and increases during dehydrogenation, indicating that the HIVC effect is still the dominant mechanism controlling the change of ρ in hydrogen. However, different from a sample deposited at 6 mTorr, the fractional change of ρ is low, namely just in the order of 10%. In addition, the baseline in a cyclic test is stable, and the magnitude of the change of ρ does not change.

We first refer to the AFM image of a freshly prepared film sample deposited at ϕ = 15 mTorr [Fig. 9(a)]. The film surface is rough, with a z_{RMS} of 2.04 nm as listed in Table I. It is imagined that small grains in the film are agglomerated to form defective clusters. These clusters are loosely packed together. During hydrogenation and dehydrogenation, the clusters are deformed, and the spacing between the clusters is readjusted, such that the internal stresses created from the phase transitions can be released effectively. This mechanism prevents severe cracking of the film structure. The AFM image taken after six switching cycles [Fig. 9(b)] supports this conjecture, where just small cracks are merely seen. The surface roughness is increased to 13.5 nm (Table I). This structure allows the HIVC effect to dominate, but the magnitude of the H-induced resistive response would be much smaller than that of a film deposited at ϕ = 6 mTorr. The actual profiles of the two cases are shown in Figs. 9(c) and 9(d) to support the above argument. Furthermore, the baseline as well as the magnitude of the fractional change in a cyclic test would be stable.

IV. CONCLUSIONS

In conclusion, Pd films were prepared by applying magnetron sputtering techniques at pressures ϕ varying from 2 to 15 mTorr. The range of mean free path of particles corresponds to a pressure range that can cover the target-to-substrate distance used in this study.

The variation of ϕ was found to be able to affect the film structure greatly. At a low ϕ environment, e.g., 2 mTorr, particles are less scattered in vacuum such that they can bombard the substrate surface with an average kinetic energy in the order of a few tens of eV. The film structure thus produced is dense and contains compressive stresses with a smoother surface. The response of ρ to H_2 is dominated by the difference between the electrical resistivities of the Pd metal phase and a hydride phase, in which volume fractions are varied during hydrogenation and dehydrogenation. The magnitude of fractional change is small, namely below 2%.

Films prepared at a moderate ϕ environment, e.g., 6 mTorr, have a defective and weak structure. Cracks are created in the film structure after several hydrogenation/dehydrogenation cycles. The cracks are responsible for huge resistive response in the presence of H_2 due to the HIVC effect. The phenomenon is considered to be very useful in hydrogen detection, if some techniques are introduced to suppress the instability and diversification of the resistive response.

The use of higher ϕ ≥ 10 mTorr produces more defective film structure with lower internal stresses and material strength. Although the HIVC effect still dominates the change of ρ, the response is weak compared with that of a film prepared at 6 mTorr.

ACKNOWLEDGMENTS

The work described in this article was substantially supported by a grant from the Research Grants Council of the Hong Kong Administrative Region (Project No. PolyU 5256/06E, account code: B-Q04J) and an internal grant from the Hong Kong Polytechnic University.

REFERENCES

1. S. Mubeen, T. Zhang, B. Yoo, M.A. Deshusses, and N.V. Myung: Palladium nanoparticles decorated single-walled carbon nanotube hydrogen sensors. *J. Phys. Chem. C* **111,** 6321 (2007).
2. Z. Zhao, M. Knight, S. Kumar, E.T. Eisenbraun, and M.A. Carpenter: Humidity effects on Pd/Au-based all-optical hydrogen sensors. *Sens. Actuators, B* **129,** 726 (2008).
3. L.L. Jewell and B.H. Davis: Review of absorption and absorption in the hydrogen-palladium system. *Appl. Catal., A* **310,** 1 (2006).
4. T. Kiefer, F. Favier, O. Vazquez-Mena, G. Villanueva, and J. Brugger: A single nanotrench in a palladium microwire for hydrogen detection. *Nanotechnology* **19,** 125502 (2008).
5. F.A. Lewis: *The Palladium Hydrogen System* (Academic Press, New York, 1967), p. 15.
6. F.A. Lewis: *The Palladium Hydrogen System* (Academic Press, New York, 1967), p. 51.
7. C. Christofides and A. Mandelis: Solid-state sensors for trace hydrogen gas detection. *J. Appl. Phys.* **68,** R1 (1990).
8. M.K. Kumar, M.S.R. Rao, and S. Ramaprabhu: Structural, morphological and hydrogen sensing studies on pulsed laser deposited nanostructured palladium thin films. *J. Phys. D: Appl. Phys.* **39,** 2791 (2006).
9. F.A. Lewis: *The Palladium Hydrogen System* (Academic Press, New York, 1967), p. 142.
10. E.A. Owen and J.I. Jones: The effect of pressure and temperature on the occlusion of hydrogen by palladium. *Proc. Phys. Soc.* **49,** A587 (1937).
11. J.C. Barton, I. Woodward, and F.A. Lewis: Hysteresis of relationships between electrical resistance and hydrogen content of palladium. *Trans. Faraday Soc.* **59,** 1201 (1963).
12. Y. Sakamoto and I. Takashima: Hysteresis behaviour of electrical resistance of the Pd–H system measured by a gas-phase method. *J. Phys.: Condens. Matter* **8,** 10511 (1996).
13. F. Favier, E.C. Walter, M.P. Zach, T. Benter, and R.M. Penner: A pyrolytic, carbon-stabilized, nanoporous Pd film for wide-range H_2 sensing. *Science* **293,** 2227 (2001).

14. O. Dankert and A. Pundt: Hydrogen-induced percolation in discontinuous films. *Appl. Phys. Lett.* **81,** 1618 (2002).
15. T. Xu, M.P. Zach, Z.L. Xiao, D. Rosenmann, U. Welp, W.K. Kwok, and G.W. Crabtree: Self-assembled monolayer-enhanced hydrogen sensing with ultrathin palladium films. *Appl. Phys. Lett.* **86,** 203104 (2005).
16. D. Ding and Z. Chen: A pyrolytic, carbon-stabilized, nanoporous Pd film for wide-range H_2 sensing. *Adv. Mater.* **19,** 1996 (2007).
17. M.P. Tsang, C.W. Ong, N. Chong, C.L. Choy, P.K. Lim, and W.W. Hung: Mechanical and etching properties of dual ion beam deposition hydrogen-free silicon nitride films. *J. Vac. Sci. Technol., A* **19,** 2542 (2001).
18. L.A. Stelmack, C.T. Thurman, and G.R. Thompson: Review of ion-assisted deposition—Research to production. *Nucl. Instrum. Methods Phys. Res., Sect. B* **37/38,** 787 (1989).
19. T.T. Leung and C.W. Ong: Control of crystallographic structure of aluminum nitride films prepared by magnetron sputtering. *Integr. Ferroelectr.* **57,** 1201 (2003).
20. T.T. Leung and C.W. Ong: Nearly amorphous to epitaxial growth of aluminum nitride films. *Diamond Relat. Mater.* **13,** 1603 (2004).